Paper Reading No.15

Multi-Scale Deep Reinforcement Learning for Real-Time

3D-Landmark Detection in CT Scans

Sheng Lian

October 2019

1 Brief Paper Intro

- ***Paper ref:*** TPAMI 2017 , https://doi.org/10.1109/TPAMI.2017.2782687
- ***Authors:*** Doring Comaniciu et al, from Friedrich-Alexander-Universitàt Erlangen-Nürnberg in Germany (埃尔朗根-纽伦堡大学).
- ***Paper summary:*** This paper adopted a deep reinforcement learning (DRL) agent to navigate in 3D CT image for automatic landmark detection. The artificial agent learns the optimized path from any location to the target point by exploiting multi-scale image representations and maximizing the accumulated rewards of taking sequential action steps. The performances on accuracy and speed are improved dramatically.
- ***Reading motivation:*** This is a 'big' paper that introduce the application of RL in the field of medical image analysis.

2 Methods

2.1 Framework overview

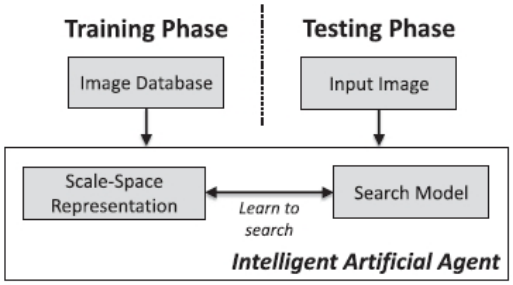

Figure 1: Schematic overview of the proposed machine learning-based paradigm for anatomical landmark detection.

This work reformulate the detection task as a behavioral problem for an artificial agent, which exploits the scale space representation of a given image. In other words, an artificial agent learns how to search for an anatomical structure.

Given that this paper is a top journal paper, there are a large amount of recap issues, including deep learning recap, the deep reinforcement learning recap, etc. These issues take almost two pages.

2.2 Method Detail

For the agent, six possible actions are indicated in Fig 2.

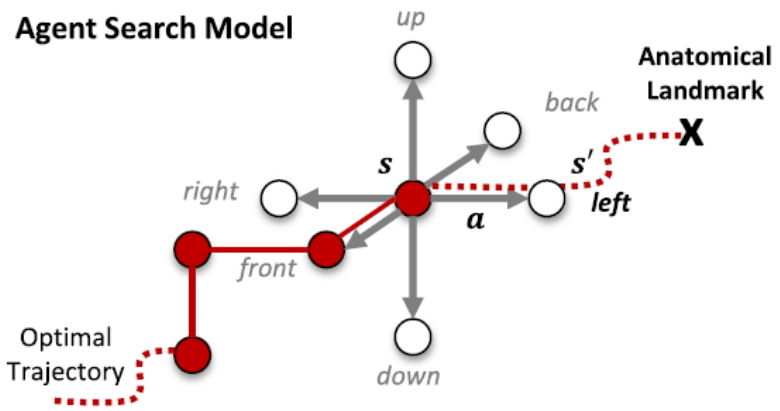

Figure 2: Schematic visualization of the decision-based search model in state s.

Overall, the proposed method integrate deep learning and reinforcement learning by deep Q-network (DQN), and use $Q(s,a;\theta) \approx Q^*(s,a)$ as a non-linear approximater for the optimal action-value function, where $\theta = [W, b]$ are the parameters of the network. The $Q(s,a;\theta)$ is formulated by the Bellman optimality equation, which goes as

$$\begin{aligned} Q^*(s,a) &= \sum_{s'} \mathcal{T}_{s,a}^{s'} \left(\mathcal{R}_{s,a}^{s'} + \gamma \max_{a'} Q^*\left(s', a'\right) \right) \\ &= \mathbb{E}_{s'} \left(r + \gamma \max_{a'} Q^*\left(s', a'\right) \right) \end{aligned} \tag{1}$$

So the expected target value can be approximate as

$$y = r + \gamma \max_{a'} Q\left(s', a'; \bar{\theta}^{(i)}\right) \tag{2}$$

The error function at each training step i is defined as

$$\hat{\theta}^{(i)} = \arg\min_{\theta^{(i)}} \mathbb{E}_{s,a,r,s'} \left[\left(y - Q\left(s, a; \theta^{(i)}\right) \right)^2 \right] \tag{3}$$

Rather than scanning the volumetric space exhaustively like other methods, the proposed method can drive the agent to effectively search for objects

in the image, through the guidance of the action-value function Q^*. Here, $\epsilon - greedy$ is adopt as an off-policy approach, and the ϵ is set to anneal linearly from 1.0 to 0.05. Also, the concept of experience replay is used, and an adaptive episode length is adopted.

2.3 Learning Multi-Scale Search Strategies

Now here is one tricky issue: how to choose the state space S, more specifically to the size of the acquired state representation? Too small or too big has their own limitation. This trade-off indicates the inability of the approach to properly exploit the image information at different scales.

The proposed method choose scale-space theory to solve the above mentioned problem. Here, the visual processing information at different scales is obtained by continuously changing the scale parameters, and then the information is integrated to deeply explore the essential features of the image. So the Q^* can be redefined as

$$Q^*(s, a|L, t) = \mathbb{E}_{s'}\left(r + \gamma \max_{a'} Q^*\left(s', a'|L, t'\right)\right) \tag{4}$$

where the scale-space representation L and the current scale level t is added. This paper finds that training a different model on each scale yields optimal results. The visualization of the detection is shown in Fig 3. On each scale,the agent navigates until convergence. And this convergence point is set as the start point of the next scale. In this paper, 3 level scales (4mm, 8mm, 16mm) are chosen.

The algorithm Fig 4 described the training steps the method.

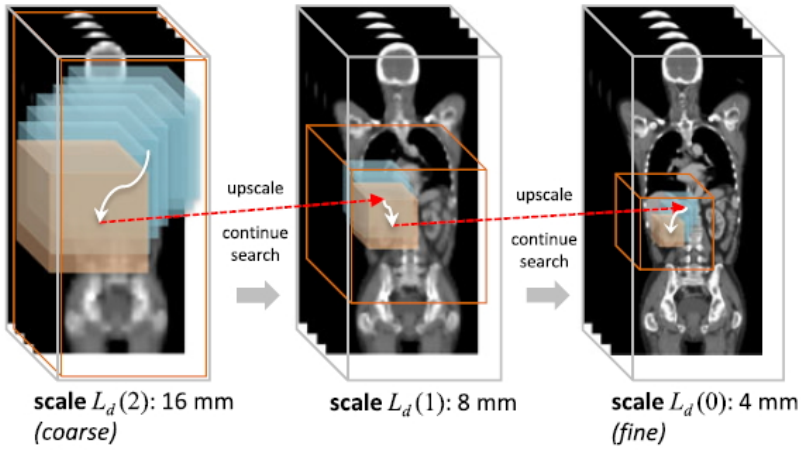

Figure 3: Visualization of the detection pipeline for the right kidney.

Algorithm 1. Training Multi-Scale DRL for Detection

Given N training 3D-CT scans: $\mathbf{I}_1, \mathbf{I}_2, \ldots, \mathbf{I}_N$
Define discrete scale-space: $L_d(t)|_{0 \leq t < M}$
Initialize system memory: $\mathbf{M}(0, \ldots, M-1) = [\,]$
Initialize exploration factor: $\epsilon = 1.0$
Initialize model parameters $\theta_t|_{0 \leq t < M}$ randomly
while $\epsilon > 0.05$ **do**
  for all scale levels $0 \leq t < M$ **do**
    Select random image and starting-point
    Sample ϵ-greedy path T with $Q(\cdot, \cdot; \theta_t \mid L_d, t)$
    $\mathbf{M}(t) \leftarrow \mathbf{M}(t) \cup [T]$
    Train $Q(\cdot, \cdot; \theta_t \mid L_d, t)$ according to Equation (12)
  end for
  Decay ϵ - reduce randomness
end while
Output $\Theta = \left[\hat{\theta}_0, \hat{\theta}_1, \ldots, \hat{\theta}_{M-1}\right]$ - estimated models

Figure 4: Algorithm 1. Training Multi-Scale DRL for Detection.

3 Experiments

The dataset used in this paper contains 1487 3D-CT volumes from 532 patients. The 8 landmarks chosen in the experiment is shown in Fig 5.

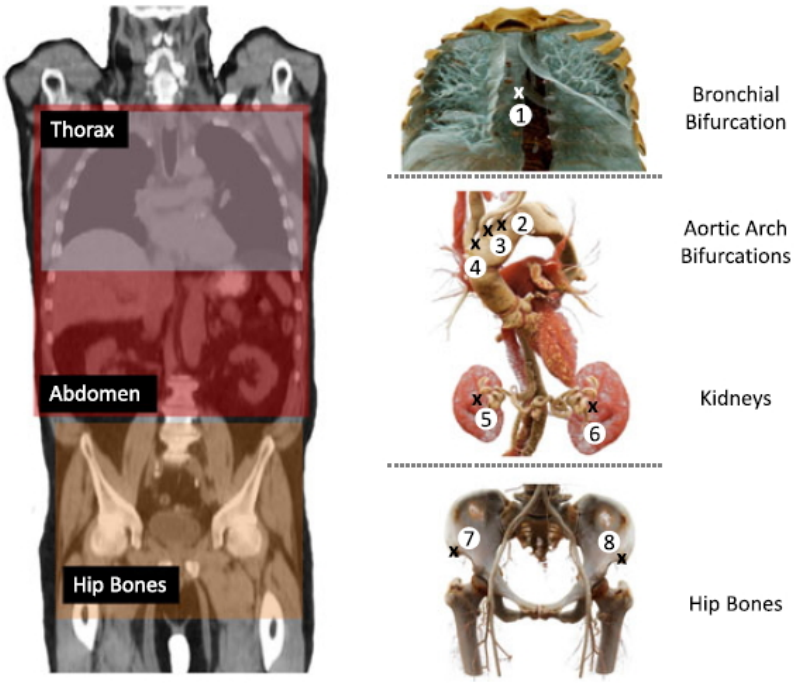

Figure 5: Visualization of all anatomical landmarks used for evaluation..

The comparison of the proposed method and other competitive approaches on accuracy and speed are shown in Fig 6. These results shows that the proposed method can achieve competitive results while significantly improve speed.

Solution	Dataset Size (Data/Patients)	Accuracy (mm)	Speed (seconds)
Zhan et al. [27]	18/18 CT	4.72	4
Fenchel et al. [35]	31/31 MR	22.4	20
Criminisi et al. [12]	100/– CT	17.60	1
Pauly et al. [32]	33/33 MR	14.95	0.8
Cuingnet et al. [11]	233/89 CT	10.5	2.8
Donner et al. [10]	20/20 CT	5.25	120
Criminisi et al. [31]	400/– CT	13.50	4
Chu et al. [30]	10/10 CT	1.90[1]	30
Potesil et al. [37]	83/83 CT	4.70	N/A
de Vos et al. [24]	100/– CT	4.80	10
Ours	**1487/532 CT**	**4.19**[2]	**0.061**

Figure 6: Table Showing a General Comparison Against Different Solutions for Anatomical Landmark Detection in Large High-Resolution Scans.

4 Conclusion

This paper proposed a DQN-based method for 3D anatomical landmark detection in CT scans. The scale issues and some outlier situation are considered. It's an extension of a MICCAI2016 paper, to the top journal TPAMI. So, the introduction of the method in the paper is very detailed, and the experiments are very solid.